Accepted Manuscript

Direct production of $TiAl_3$ from Ti/Al-containing oxides precursors by solid oxide membrane (SOM) process

Shangshu Li, Xingli Zou, Kai Zheng, Xionggang Lu, Qian Xu, Chaoyi Chen, Zhongfu Zhou

PII: S0925-8388(17)32942-0

DOI: 10.1016/j.jallcom.2017.08.213

Reference: JALCOM 42970

To appear in: *Journal of Alloys and Compounds*

Received Date: 29 November 2016

Revised Date: 20 August 2017

Accepted Date: 22 August 2017

Please cite this article as: S. Li, X. Zou, K. Zheng, X. Lu, Q. Xu, C. Chen, Z. Zhou, Direct production of $TiAl_3$ from Ti/Al-containing oxides precursors by solid oxide membrane (SOM) process, *Journal of Alloys and Compounds* (2017), doi: 10.1016/j.jallcom.2017.08.213.

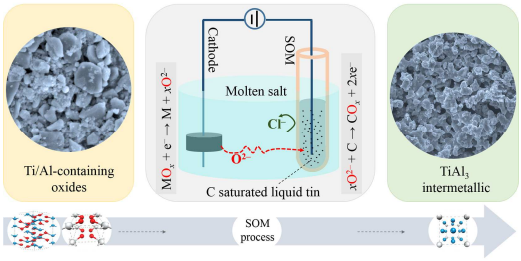

Direct production of $TiAl_3$ from Ti/Al-containing oxides precursors by solid oxide membrane (SOM) process

Shangshu Li [a], Xingli Zou [a,b,*], Kai Zheng [a], Xionggang Lu [a,*] Qian Xu [a], Chaoyi Chen [c], Zhongfu Zhou [a,d]

a. State Key Laboratory of Advanced Special Steel & Shanghai Key Laboratory of Advanced Ferrometallurgy & School of Materials Science and Engineering, Shanghai University, Shanghai 200072, China

b. Center for Electrochemistry, Department of Chemistry, The University of Texas at Austin, Austin, 78712, Texas, US

c. School of Materials and Metallurgy, Guizhou University, Guiyang 550025, China

d. Institute of Mathematics and Physics, Aberystwyth University, Aberystwyth, SY23 3BZ, UK

*Corresponding author, E-mail: xinglizou@shu.edu.cn (X. Zou), luxg@shu.edu.cn (X. Lu)

Abstract

$TiAl_3$ intermetallic has been successfully synthesized by the electrochemical deoxidation of the Ti/Al-containing oxides precursors including TiO_2/Al_2O_3 mixture and titanium-rich slag/Al_2O_3 mixture at 1000 °C and 3.8 V in molten $CaCl_2$. A solid oxide membrane (SOM) tube filled with carbon-saturated liquid tin was served as inert anode, and the pressed pellet of Ti/Al-containing oxides precursors was used as cathode during the electrochemical deoxidation process. The results show that the reduction proceeds through a serious of individual stages, which mainly involve the formation-decomposition of calcium titanium/aluminum oxides and the formation of

$TiAl_x$ alloys. The analysis of the partially reduced cathode pellet confirms that the three phases interlines (3PIs) reaction area gradually expands from the pellet's surface to its centre. The morphology of the $TiAl_3$ obtained from TiO_2/Al_2O_3 precursor exhibits a homogeneous nodular structure. The final product produced from the titanium-rich slag/Al_2O_3 precursor contains $TiAl_3$ and Ll_2 $Ti_{0.75}Fe_{0.25}Al_3$. In addition, the porous $TiAl_3$ with high porosity can be prepared by using NaCl as the space-holder material. The results demonstrate that the SOM process has the potential to be used for the facile production of Ti-Al alloys from complex oxides precursors.

Keywords: $TiAl_3$; electro-deoxidation; SOM; oxides; $CaCl_2$

1 Introduction

Titanium aluminides (includes Ti_3Al, TiAl and $TiAl_3$) are regarded as innovative high-temperature engineering materials owing to their excellent properties [1-3]. Among these titanium aluminides, $TiAl_3$ is the most lightest with a density of ~3.4 g/cm^3 [4]. Moreover, good oxidation, high modulus of elasticity, moderately high melting temperature (around 1400 °C) and conceivable high-temperature specific strength make $TiAl_3$ becomes an attractive potential candidate for aerospace application [5-7]. In addition, $TiAl_3$ is a suitable reinforcement for aluminum due to the good wettability and clean interface between $TiAl_3$ and Al matrix [8]. Numerous technologies have been developed to prepare $TiAl_3$ from Ti and Al powders, such as arc melting, thermal explosion (TE), hot pressing (HP) and reaction synthesis of solid Ti and liquid Al [9-14]. The process (usually Kroll process) used for producing Ti powder generally involves high cost and high energy consumption.

In 2000, a novel electrochemical deoxidation method named FFC Cambridge process has been first proposed to extract metals and alloys directly from metal oxides [15]. The electrochemical deoxidation process is commonly operated at a moderate temperature (800–1000 °C) in molten salts, such as molten LiCl, $CaCl_2$ and $CaCl_2$-NaCl [16, 17]. During the electrochemical deoxidation process, the inexpensive metal oxides are used as raw materials, and the metals/alloys/composites can be directly synthesized at cathode. Generally, the graphite is used as the consumable anode during electro-deoxidation to react with O^{2-} to form CO and/or CO_2 gas. The generated CO_2 can further react with O^{2-} in the molten electrolyte to form CO_3^{2-} ($CO_2 + O^{2-} \rightarrow CO_3^{2-}$). Consequently, C can be formed through the side electrochemical reaction ($CO_3^{2-} + 4e^- \rightarrow C + 3O^{2-}$) and thus influence the deoxidation process [18, 19]. In addition, the graphite powder dropped from the graphite anode will also pollute the molten salts and inevitably decrease the current efficiency of the electrochemical deoxidation process [20]. However, these side reactions and carbon pollution can be avoided by modifying the consumable anode. The solid oxide membrane (SOM) assembled anode system has been proved can be used as the inert anode to replace the graphite anode [21, 22]. During the SOM-assisted electro-deoxidation process, only O^{2-} can pass through the SOM and thus the anodic reaction area has been separated from the molten salts, as schematically shown in Fig. 1 [22-24]. Generally, high current efficiency can be achieved by using the SOM-assisted electro-deoxidation process due to the carbon-related side reactions have been avoided [25]. In the previous work [22, 24-30], various

metals/alloys/composites have been successfully synthesized from their relevant oxides and complex ores (such as titanium-rich slag, ilmenite and Ti-bearing blast-furnace slag) by using the SOM-assisted electro-deoxidation method. The SOM process has been considered as a green and effective technology for the preparation of metals/alloys/composites, especially refractory materials [30].

The melting point of aluminum is only 660 °C, theoretically, aluminum is liquid at the experimental temperature (800–1000 °C) during the electrochemical deoxidation process. However, aluminum can react with Ti to form Ti-Al alloys during the solid-state electro-deoxidation process [31]. In the present study, $TiAl_3$ intermetallic has been electrochemically synthesized from TiO_2/Al_2O_3 precursor and titanium-rich slag/Al_2O_3 precursor in molten $CaCl_2$ by using the SOM-assisted electro-deoxidation process. The phase composition of the cathodic products obtained from different electrolysis conditions was systematically investigated by using X-ray diffraction (XRD), and the microstructure of the final product was analyzed by using scanning electron microscope (SEM). In addition, the phase composition of the partially reduced pellet has been carefully analyzed by using XRD from the pellet's surface to its centre area, and the reaction pathway during the electrochemical deoxidation process of Ti/Al-containing oxides precursors in molten $CaCl_2$ has been discussed. In addition, the porous $TiAl_3$ alloy has also been tried to electrochemically produce by the SOM process with the use of NaCl as a space-holder material.

2 Experimental

2.1 Fabrication of electrodes

The raw materials used in the experiments involve commercial TiO_2, Al_2O_3 and titanium-rich slag. The titanium-rich slag was produced by the reduction of the titaniumferrite ore with coal in an electric arc furnace, and the chemical composition of the slag is listed in Table 1. The mixture of TiO_2 and Al_2O_3 was prepared at the stoichiometric ratio of Ti:Al = 1:3 (34.31 wt % TiO_2 and 65.69 wt % Al_2O_3) corresponding to $TiAl_3$. Then, the TiO_2/Al_2O_3 mixture with anhydrous alcohol and 5 wt % polyvinyl butyral (PVB) was ball-milled for about 4 h at a rotation rate of 450 r/min. The milled mixture was then pressed under a stable pressure (12 MPa) for 2 min to form a cylinder pellet. In addition, the titanium-rich slag/Al_2O_3 mixture (49.91 wt % titanium-rich slag and 50.09 wt % Al_2O_3) pellet was also prepared using the above process. The pressed pellet without being pre-sintered in high temperature has been proved to possess enough strength to meet the requirement of electrolysis. The pressed pellet was directly sandwiched between two porous nickel foils, and then fixed with Fe-Cr-Al alloy wire (1.5 mm in diameter) to form a cathode. The porous nickel foil can provide more initial reduction points to the mixture pellet during the early stage of electrolysis.

The SOM tube (8 mol % yttria-stabilized zirconia (YSZ)) used in the experiment was fabricated by slip casting and high temperature sintering process. It has been proved that the home-made SOM tube can support a long time electrolysis process [25, 27-29]. The inert anode was composed of the SOM tube filled with carbon-saturated liquid tin, and a Fe-Cr-Al/Mo wire was inserted into the tube to conduct electric current. The liquid tin contained in the SOM tube is acted as a

medium to transport O^{2-} generated from the electrochemical reduction reactions, *i.e.*, $MO_x + 2xe^- \rightarrow M + 2xO^{2-}$. The carbon saturated in liquid tin is used as reductant to react with oxygen ions, *i.e.*, $C + xO^{2-} \rightarrow CO_{x(x=1 \text{ or } 2)} + 2xe^-$. As shown in Fig. 1, the key feature of the SOM-assisted electro-deoxidation process is that the anode reaction area can be separated by the SOM tube from the molten salt, therefore, only O^{2-} can pass through the SOM tube. As a result, the CO/CO_2 generated in the SOM tube cannot react with O^{2-} in the molten electrolyte to form CO_3^{2-}, and thus the carbon-related side reactions can be effectively avoided. In addition, higher voltage (such as 3.5–4.0 V [29],) can be applied during the SOM-assisted electro-deoxidation process, which means that the SOM electrolysis process generally possesses high reduction speed [25].

2.2 Electrolysis procedure

The assembled cathode and anode were placed in a corundum crucible which contained molten $CaCl_2$ as electrolyte. The experiments were systematically carried out in a vertical tubular corundum reactor which was located in an electrical furnace, as shown in Fig. 1. The ultra-purity argon gas was continuously purged into corundum reactor to provide/keep an inert atmosphere during the electrochemical deoxidation process. The electrochemical experiments include the pre-electrolysis of molten $CaCl_2$ and the subsequent electrochemical deoxidation process. The pre-electrolysis with the aim to remove residual redox-active species and residual moisture from molten $CaCl_2$ was performed at 2.5 V and 1000 °C between a Fe-Cr-Al alloy wire cathode and the SOM anode for 2 h. The electrochemical deoxidation process was then conducted at

3.8 V and 1000 °C between the pellet cathode and the SOM anode for appropriate time. A BioLogic HCP-830 electrochemical workstation was used to control the electrochemical experiment. After the electrolysis was finished, the reduced cathode was taken out from corundum reactor, washed with tap water and dried at 90 °C in a drying oven.

2.3 Characterization

The chemical composition of the titanium-rich slag was analyzed by X-ray fluorescence spectroscopy (XRF-1800, Shimadzu Limited Co. Japanese) and inductive-coupled plasma spectroscopy (ICP, Perkin Elmer PE400). The phase composition of the cathodic products was determined by a D8 Advance X-ray diffractometer (XRD, Bruker Co. Germany). The morphology of the cathodic products was examined by scanning electron microscopy (SEM) on a JEOL JSM-6700F microscope. The elemental composition of the cathodic products was analyzed by energy-dispersive X-ray (EDX) spectroscopy (Oxford INCA EDS system) attached to the SEM.

3 Results and discussion

3.1 Production of $TiAl_3$ from TiO_2/Al_2O_3 mixture precursor

3.1.1 XRD analysis

To investigate the influence of molten $CaCl_2$ immersion process on the precursors, the TiO_2/Al_2O_3 mixture pellet was immersed in molten $CaCl_2$ bath (without being pre-electrolyzed) at 1000 °C for 2 h. As presented in Fig. 2, the phase composition of the pellet after being immersed in molten $CaCl_2$ for 2 h mainly

contains Al_2O_3, $Ca_{12}Al_{14}O_{33}$ and $CaTiO_3$. This finding suggests that TiO_2 and Al_2O_3 are converted mostly into $CaTiO_3$ and $Ca_{12}Al_{14}O_{33}$ through chemical reaction processes. Actually, a small amount of CaO would inevitably exist in molten $CaCl_2$ due to the impurity of the purchased $CaCl_2$ (purity ≥ 98 %). In addition, CaO is believed to be available in molten $CaCl_2$ salt due to the hydrolysis reaction of $CaCl_2{\cdot}x(H_2O)$, *i.e.*, $CaCl_2{\cdot}H_2O \rightarrow CaO + 2HCl$ [32]. Therefore, the chemical formation of $CaTiO_3$ and $Ca_{12}Al_{14}O_{33}$ can take place by reactions (1) and (2).

$$TiO_2 + CaO \rightarrow CaTiO_3 \qquad \Delta G^{\theta}_{(1000\ ^{\circ}C)} = -88.36\ \text{kJ/mol} \qquad (1)$$

$$7Al_2O_3 + 12CaO \rightarrow Ca_{12}Al_{14}O_{33} \qquad \Delta G^{\theta}_{(1000\ ^{\circ}C)} = -374.97\ \text{kJ/mol} \qquad (2)$$

In order to investigate the detailed variations of phase composition during the electrochemical deoxidation process, the partially reduced pellets obtained from different electrolysis times were systematically analyzed. As revealed in Fig. 3, Al_2O_3, $Ca_{12}Al_{14}O_{33}$ and $CaTiO_3$, along with trace amount of Ti_3O_5 were obtained after 1 h electrolysis. During the electrochemical deoxidation process, oxygen was continuously removed from the cathode to molten $CaCl_2$. Hence, the chemical reactions between TiO_2/Al_2O_3 and O^{2-}/Ca^{2+} will also contribute to the formations of $CaTiO_3$ and $Ca_{12}Al_{14}O_{33}$, as expressed by reactions (3) and (4). Besides Al_2O_3, $Ca_{12}Al_{14}O_{33}$ and $CaTiO_3$, the titanium sub-oxides Ti_2O_3 and TiO have also been found to coexist in the product obtained from electrolysis for 2 h. When the electrolysis time was prolonged to 3 h, a small amount of TiAl was generated, however, the main phases still consisted of Al_2O_3, $Ca_{12}Al_{14}O_{33}$ and $CaTiO_3$. The decomposition potentials of Al_2O_3, $Ca_{12}Al_{14}O_{33}$ and $CaTiO_3$ at 1000 °C are calculated to be 2.18 V,

2.27 V and 2.07 V, respectively. Obviously, $Ca_{12}Al_{14}O_{33}$ is a relatively stable compound during the electrochemical deoxidation process [29]. As revealed in Fig. 3, a certain amount of $Ca_{12}Al_{14}O_{33}$ still existed in the pellet after being electrolyzed for 4 h. Besides, $TiAl_2$ and $TiAl_3$ were formed through the reactions between the generated titanium and aluminum. The product obtained from electrolysis for 5 h contained $TiAl_3$, $TiAl_2$, Al_2Ti_3 and Al_2O_3. $TiAl_3$ was finally formed when the electrolysis time was extended to 6 h. The observation of the intermediates $CaTiO_3$, Ti_3O_5, Ti_2O_3 and TiO suggests that the electrochemical deoxidation of TiO_2 is a multi-step process as the sequence: $TiO_2 \rightarrow CaTiO_3 \rightarrow Ti_3O_5 \rightarrow Ti_2O_3 \rightarrow TiO \rightarrow Ti$ and/or $TiO_2 \rightarrow Ti_3O_5 \rightarrow Ti_2O_3 \rightarrow TiO \rightarrow Ti$. In addition to the direct reduction of Al_2O_3, partial Al_2O_3 was firstly converted into $Ca_{12}Al_{14}O_{33}$ and then reduced to Al. The formed titanium and aluminum would react to form $TiAl_x$ (Al_2Ti_3, TiAl, $TiAl_2$ and $TiAl_3$) in the cathode according to reactions (5)–(8), and $TiAl_3$ was finally formed with the increase of electrolysis time.

$$TiO_2 + Ca^{2+} + O^{2-} \rightarrow CaTiO_3 \quad (3)$$

$$7Al_2O_3 + 12Ca^{2+} + 12O^{2-} \rightarrow Ca_{12}Al_{14}O_{33} \quad (4)$$

$$3Ti + 2Al \rightarrow Al_2Ti_3 \quad (5)$$

$$Al_2Ti_3 + Al \rightarrow 3TiAl \quad (6)$$

$$TiAl + Al \rightarrow TiAl_2 \quad (7)$$

$$TiAl_2 + Al \rightarrow TiAl_3 \quad (8)$$

Generally, the reduction process gradually extends from the pellet's surface to its interior. To further investigate the detailed electrochemical deoxidation process for

TiO_2/Al_2O_3 mixture pellet, a partially reduced pellet was analyzed by XRD. In this experiment, the partially reduced pellet was ground from the pellet's surface to its interior in a certain distance, as illustrated in Fig. 4a. Then the phase composition of the corresponding layers was determined by XRD, as shown in Fig. 4b. As revealed in the figure, the pellet's surface has been completely reduced to $TiAl_3$. However, the pellet's centre still contains unreduced oxides/compounds (Al_2O_3, $Ca_{12}Al_{14}O_{33}$, $CaTiO_3$ and Ti_2O_3), and the formation of Ti_2O_3 may be attributed to the reduction of $CaTiO_3$ and/or TiO_2. The aluminum-containing oxide compounds $CaAl_4O_7$ and $Ca_{12}Al_{14}O_{33}$ exist in the pellet's exterior and interior, respectively. $CaAl_4O_7$ may be formed through the reduction of $Ca_{12}Al_{14}O_{33}$ and/or the combination reaction of Al_2O_3 with Ca^{2+} and O^{2-}, as described in reactions (9) and (10). It can be seen that the Ti-containing oxides (Ti_2O_3 and $CaTiO_3$) exist in the centre of the pellet, and no Ti-containing oxides present in the outer of the pellet. The decomposition potentials of Ti-containing oxides (Ti_2O_3: 2.02 V; $CaTiO_3$: 2.07 V) are lower than that of Al-containing oxides ($Ca_{12}Al_{14}O_{33}$: 2.27 V; $CaAl_4O_7$: 2.25 V; Al_2O_3: 2.18 V). Therefore, titanium can be facilely formed during the electrochemical deoxidation process. It is worth nothing that the formed aluminum may also be beneficial to the reduction of titanic oxides through an aluminothermic reduction process such as $Ti_2O_3 + 2Al \rightarrow 2Ti + Al_2O_3$ ($\Delta G^{\theta}_{(1000\,^{\circ}C)} = -99.954$ kJ/mol). The formed aluminum will react with titanium to generate $TiAl_x$ $(x < 3)$ intermetallics, *i.e.*, Ti_2Al, Ti_3Al_2, TiAl and $TiAl_2$. Eventually, $TiAl_3$ can be formed by the reaction of $TiAl_2$ and Al when enough aluminum is produced. Therefore, the partially reduced pellet can be divided into

three parts, *i.e.*, surface (completely reduced part), middle layer (partially reduced part) and centre (unreduced part). The phase composition of each part is summarized in Fig. 4c, in which the xCaO·yAl$_2$O$_3$ mainly refers to $Ca_{12}Al_{14}O_{33}$ and $CaAl_4O_7$.

$$2Al_2O_3 + CaO \rightarrow CaAl_4O_7 \qquad \Delta G^{\theta}_{(1000\ ^{\circ}C)} = -58.67\ \text{kJ/mol} \tag{9}$$

$$Ca_{12}Al_{14}O_{33} + 30e^- \rightarrow 11CaO + 10Al + CaAl_4O_7 + 15O^{2-} \qquad E_{(1000\ ^{\circ}C)} = 2.30\ \text{V} \tag{10}$$

3.1.2 Morphology observation

During the electrochemical deoxidation process, it is well determined that the reduction reaction occurs at the oxides/molten salt/metal three–phase interlines (3PIs) area [33, 34]. The 3PIs are firstly formed on the surface of pellet and then gradually expands along the depth direction. Fig. 5a shows the SEM image of the section of a ground pellet electrolyzed for 3 h. As evidenced in the figure, the pellet has not been completely reduced. It is clear that the section of pellet shows different morphologies, and it consists of two parts separated by the 3PIs. The outer part shows a loose and homogeneous morphology (Fig. 5a and g), on the contrary, the inner part possesses a dense structure (Fig. 5a and h). It should be noted that the loose structure can provide the direct channels for the transmission of molten $CaCl_2$ and the migration of oxygen ions during the electrochemical deoxidization process. The corresponding elemental analysis indicates that the outer part has been almost reduced to Ti-Al alloys, whereas the inner part is still unreacted, as revealed in Fig. 5c–f. According to the EDX analysis presented in Fig. 5b, a considerable amount of elements Ca and O, along with elements Ti and Al, exist in the inner part of the pellet, which mainly correspond to the intermediate compounds, *i.e.*, $CaTiO_3$, $Ca_{12}Al_{14}O_{33}$, $CaAl_4O_7$, *etc*. As the

electrolysis time increasing, these intermediate compounds would be reduced to titanium and aluminum respectively. As a result, the dense structure of the inner part would also become loose/porous.

Fig. 6 shows the SEM images of the product electrolyzed for 6 h. The EDX analysis suggests that the TiO_2/Al_2O_3 mixture has been completely reduced to $TiAl_3$ alloy. As revealed in the Fig. 6a, the obtained $TiAl_3$ particles possess a uniform microstructure and these $TiAl_3$ particles (approximately 3–5 μm) begin to interconnect with each other to form a porous nodular structure. Actually, the interconnected $TiAl_3$ particles are grew up from the smaller particles (approximately 1 μm) through the sintering process, as evidenced in Fig. 6b. It should be noted that the formed aluminum is theoretically presented in liquid form at the experimental temperature (1000 °C, the melting point of Al is 660 °C). However, the liquid Al can react with the surrounded/generated titanium to form Ti-Al intermetallics immediately. Meanwhile, the liquid Al may also act as the binder to accelerate the sintering of the surrounding solid particles.

3.1.3 Synthesis of porous $TiAl_3$

It was suggested that the titanium alloys with a predesigned geometry can be prepared *via* the reduction of the pre-formed oxide precursors in molten salts [35]. Porous $TiAl_3$ intermetallic can be applied as heat insulation and separation materials due to its better oxidation resistance in elevated temperature [36, 37]. Therefore, we tried to electrochemically prepare porous $TiAl_3$ from the TiO_2/Al_2O_3 mixture precursor with a space-holder material (NaCl) in molten $CaCl_2$. The whole

experimental process is illustrated in Fig. 7. NaCl particles (200–500 μm) are used as the space-holder material, which can be removed easily from the pellet by dissolving into molten $CaCl_2$ at experimental temperature (1000 °C). Fig. 8 presents the SEM images of the final $TiAl_3$ obtained from different electrolysis conditions. Obviously, there are lots of tiny pores (marked with arrows in Fig. 8a and d) are found among the interconnected nodular skeletons due to the reduction and the sintering processes. In addition, it is obvious that the microstructures of the electrolyzed pellets with/without NaCl show considerable difference, as shown in Fig. 8a and Fig 8b, c. The large pores are distributed on the skeletons (marked with circles in Fig. 8b and c), the pore sizes are approximately 100-500 μm. Evidently, the large pores are formed because of the removal of initial NaCl particles during the electrochemical deoxidation process. It should be noted that the pore size and porosity of the porous $TiAl_3$ can be affected by the characteristics of the added NaCl particles, such as particle size, shapes and contents [37].

3.1.4 Reaction mechanism of the electrochemical deoxidation process

Based on the time/position-dependent variations of phase composition (Figs. 2–4), the thermodynamic consideration (at 1000 °C), and the previous studies on the reaction mechanisms of the electrochemical reduction of metal oxides [19, 29, 38-40], the reaction path of electrochemical reduction of TiO_2/Al_2O_3 mixture precursor to $TiAl_3$ in molten $CaCl_2$ has been suggested, as schematically illustrated in Fig. 9. It is suggested that the electrochemical synthesis of $TiAl_3$ mainly includes three parts, *i.e.*, the formation-decomposition of Ti-containing oxides, the formation-decomposition of

Al-containing oxides and the formation of $TiAl_x$. The formation of $CaTiO_3$ is inevitable due to the reaction of TiO_2 and $CaO/(Ca^{2+}, O^{2-})$ during the electrochemical deoxidation process, as described in reactions (1) and (3). The decomposition of $CaTiO_3/TiO_2$ proceeds through a number of individual steps which mainly involve the formation and reduction of $Ti_{x-1}O_{2x-3}$ (*i.e.*, Ti_3O_5, Ti_2O_3 and TiO) (reactions (11)–(13)) [19, 40]. The dissolubility of CaO in molten $CaCl_2$ is approximately 21 mol % [41], therefore, the generated CaO can completely dissolve into molten $CaCl_2$.

$$3TiO_2/CaTiO_3 + 2e^- \rightarrow Ti_3O_5/2CaO + O^{2-} \quad E_{(1000\,^\circ C)} = 1.28\ V/2.65\ V \tag{11}$$

$$(x-2)Ti_{x-1}O_{2x-3} + 2e^- \rightarrow (x-1)Ti_{x-2}O_{2x-5} + O^{2-}$$

$$E_{(1000\,^\circ C)} = 1.46\ V\ (x = 3),\ 1.70\ V\ (x = 4) \tag{12}$$

$$TiO + 2e^- \rightarrow Ti + O^{2-} \qquad E_{(1000\,^\circ C)} = 2.18\ V \tag{13}$$

$Ca_{12}Al_{14}O_{33}$ is also formed through the chemical reactions (reactions (2) and (4)), which is similar to the formation of $CaTiO_3$. Then $Ca_{12}Al_{14}O_{33}$ can be reduced to compound $CaAl_4O_7$ according to reaction (10). Therefore, Aluminum can be formed by the reduction of Al_2O_3, $Ca_{12}Al_{14}O_{33}$ and $CaAl_4O_7$ according to reactions (14)–(16).

$$Al_2O_3 + 6e^- \rightarrow 2Al + 3O^{2-} \qquad E_{(1000\,^\circ C)} = 2.18\ V \tag{14}$$

$$Ca_{12}Al_{14}O_{33} + 42e^- \rightarrow 12CaO + 14Al + 21O^{2-} \qquad E_{(1000\,^\circ C)} = 2.27\ V \tag{15}$$

$$CaAl_4O_7 + 12e^- \rightarrow CaO + 4Al + 6O^{2-} \qquad E_{(1000\,^\circ C)} = 2.25\ V \tag{16}$$

Ti-Al intermetallics ($TiAl_x$) are formed by the reactions between titanium and aluminum and the formation process can be expressed by the reaction sequences (reactions (5)–(8)): $Ti_2Al \rightarrow Ti_3Al_2 \rightarrow TiAl \rightarrow TiAl_2 \rightarrow TiAl_3$. It should be noted that the above-mentioned formation steps are not necessarily in temporal sequence, and

they may occur simultaneously during the electrochemical deoxidization process.

3.2 Production of $TiAl_3$ from titanium-rich slag/Al_2O_3 mixture precursor

3.2.1 XRD analysis

The electrochemical synthesis of $TiAl_3$ from titanium-rich slag has also been investigated. 50.09 wt % Al_2O_3 was added into the titanium-rich slag to provide adequate aluminum to form $TiAl_3$. The variations of the phase composition during the electrochemical deoxidation process were determined by XRD, as revealed in Fig. 10. As evidenced in Fig. 10a, the initially as-received titanium-rich slag with complex composition is composed of kennedyite ($(Fe_{0.33}Ti_{0.46}Mg_{0.21})(Ti_{1.9}Mg_{0.1})O_5$, PDF# 80-1216), titanite ($CaTiSiO_5$, PDF# 73-2066) and trace amount of rutile (TiO_2, PDF#). The XRD analysis result (Fig. 10a and b) reveals that the pellet has been deoxidized completely within approximately 4–5 h. The final product contains $TiAl_3$, $Ti_{0.75}Fe_{0.25}Al_3$, and trace amount of Ti_5Si_3. A fact that Fe can be partially/completely removed during the electrochemical deoxidation process has been reported in the previous work [29, 42]. However, in this work, it is relatively difficult to completely remove Fe from the pellet during the electrochemical deoxidation process due to the content of total FeO_x in the titanium-rich slag is 12.77 wt %. Actually, the generated Fe can promote the subsequent electrochemical process due to its good electronic conductivity [27, 43], and Fe will react with Ti and Al to form $Ti_{0.75}Fe_{0.25}Al_3$ intermetallic. It should be noted that $Ti_{0.75}Fe_{0.25}Al_3$ intermetallic has the high-symmetry Ll_2 cubic structure and thus has better ductility compared to the tetragonal DO_{22} structure $TiAl_3$. Usually, the ductility of $TiAl_3$ can be improved by

alloying with other elements, such as Cr, Mn, Fe and Co [9, 10]. During the early stage of the electrochemical deoxidation process (first 1 h electrolysis), the product mainly contains unreduced oxides/compounds, *i.e.*, Al_2O_3, $CaTiO_3$, $Ca_{12}Al_{14}O_{33}$, $Ca_4Al_6O_{13}$, Ti_2O_3 and Ti_3O_5. $Ca_4Al_6O_{13}$ can be formed by the electrochemical deoxidation of $Ca_{12}Al_{14}O_{33}$ ($Ca_{12}Al_{14}O_{33} + 24e^- \rightarrow 8CaO + Ca_4Al_6O_{13} + 8Al + 12O^{2-}$) and the reaction between Al_2O_3 and $CaO/(Ca^{2+}, O^{2-})$ ($3Al_2O_3 + 4CaO/(Ca^{2+}, O^{2-}) \rightarrow Ca_4Al_6O_{13}$). Finally, the formed titanium and aluminum will react with each other to form $TiAl_2$, and then the formed $TiAl_2$ can further react with Al to form $TiAl_3$, as shown in Fig. 10 (2, 3 and 4 h).

Fig. 11 presents the XRD patterns of a partially reduced pellet (electrolyzed for 1.5 h) from the pellet's surface to its centre. The product of the interior of the pellet mainly contains unreduced oxides/compounds, *i.e.*, Al_2O_3, $Ca_{12}Al_{14}O_{33}$, $Ca_4Al_6O_{13}$, Ti_2O_3 $CaTiO_3$, TiO *etc*. Based on the experimental results (Figs. 10 and 11), the reduction pathway of Ti-containing oxides follows the sequence of $CaTiO_3 \rightarrow Ti_3O_5 \rightarrow Ti_2O_3 \rightarrow TiO \rightarrow Ti$. In addition, the reduction pathway of Al-containing oxides follows the sequences of $Al_2O_3 \rightarrow Al$ and/or $Al_2O_3 \rightarrow (Ca_{12}Al_{14}O_{33} \rightarrow Ca_4Al_6O_{13}) \rightarrow Al$. Moreover, $TiAl_2$, Al_2O_3 and Ti_5Si_3 are identified as the main phases of the surface of the pellet. Obviously, when the residual Al_2O_3 was reduced to aluminum, $TiAl_2$ would finally react with Al to form $TiAl_3$. It is obvious that the intensity of $TiAl_2$ peaks decreases while the intensity of Al_2O_3 peaks increase gradually along the depth direction. This observation is consistent with the expansion of 3PIs reaction area from the surface to the inner part of the pellet during the electrochemical deoxidation

process.

3.2.2 Morphology observation

The as-received titanium-rich slag powder shows an irregular morphology according to Fig. 12a, and the particle size is around 9 μm. The EDX analysis (the inset in Fig. 12a) over the SEM imaging area confirms that the titanium-rich slag consists of relatively complex compounds. Fig. 12b shows the SEM image of the titanium-rich slag/Al_2O_3 mixture after being ball-milled for 4 h. It is clear that the particle size of the ball-milled mixture (approximately 5 μm) is less than that of the initial titanium-rich slag. The SEM image of the completely electrolyzed product obtained after 5 h electrolysis is presented in Fig. 12c. The particles of the final product possess smooth surfaces, and the particles begin to interconnect together to form a porous sponge-like microstructure owing to the sintering affect during the electrochemical deoxidation process. Elements Ti, Al, Fe and Si (corresponding to $TiAl_3$, $Ti_{0.75}Fe_{0.25}Al_3$ and Ti_5Si_3) were found in the final product. The impurity elements Ca and Mg can be partially/completely removed through the chemical/ physical processes [29, 44, 45]. It should be noted that there are two types of morphology present in the final product, *i.e.*, the large and little particles, as evidenced in Fig. 12c. According to the EDX analysis (Fig. 12d), it is obvious that the little particles are Ti_5Si_3 and the large particles are $TiAl_3$. Ti_5Si_3 is formed through the reaction between the formed titanium and silicon according to the reaction: $5Ti + 3Si \rightarrow Ti_5Si_3$ ($\Delta G^{\theta}_{(1000\,^{\circ}C)} = -589.26$ kJ/mol).

4. Conclusions

The pressed pellets of Ti/Al-containing oxide precursors (*i.e.*, TiO_2/Al_2O_3 mixture and titanium-rich slag/Al_2O_3 mixture) have been electrochemically reduced to $TiAl_3$ intermetallic by using the SOM-assisted electro-deoxidation process in molten $CaCl_2$ at 1000 °C and 3.8 V. The characteristics of the products obtained from different electrolysis conditions were systematically investigated. The results suggest that the reaction mechanism of the electrolysis can be divided into three steps: (*i*) the compounding reaction of TiO_2, Al_2O_3 and CaO/(Ca^{2+}, O^{2-}) to form compounds $CaTiO_3$ and $Ca_{12}Al_{14}O_{33}$; (*ii*) the reduction of $CaTiO_3$ to titanium sub-oxide Ti_xO_y and titanium in sequence, and the reduction of Al_2O_3 and $xCaO{\cdot}yAl_2O_3$ (includes $Ca_{12}Al_{14}O_{33}$ and $CaAl_4O_7$) to Al; (*iii*) the formation of $TiAl_3$ through the reactions between titanium and aluminum. The systematical analyses of the partially reduced pellet demonstrate that the reduction process expands gradually from the surface to the inner of the pellet. The produced $TiAl_3$ particles obtained from TiO_2/Al_2O_3 precursor possess a typical interconnected nodular microstructure. $TiAl_3$ and Ll_2 $Ti_{0.75}Fe_{0.25}Al_3$ can be obtained from titanium-rich slag/Al_2O_3 mixture precursor. In addition, the electrochemical preparation of porous $TiAl_3$ from TiO_2/Al_2O_3 mixture precursor has also been proved by using the electrochemical deoxidation process.

Acknowledgments

This work was supported by the National Natural Science Foundation of China (Nos. 51225401, 51304132, 51574146 and 51664005), the Science and Technology Commissions of Shanghai Municipality (No. 14JC1491400), the National Basic Research Program of China (No. 2014CB643403) and the Young Teacher Training

Program of Shanghai Municipal Education Commission.

References

[1] R.G. Reddy, X. Wen, I.C.I. Okafor, Diffusion of oxygen in the Al_2O_3 oxidation product of $TiAl_3$, Metall. Mater. Trans. A 31A (2000) 3023-3028.

[2] Y. Watanabe, H. Eryu, K. Matsuura, Evaluation of three-dimensional orientation of Al_3Ti platelet in Al-based functionally graded materials fabricated by a centrifugal casting technique, Acta Mater. 49 (2001) 775-783.

[3] E.K.Y. Fu, R.D. Rawlings, H.B. Mcshane, Reaction synthesis of titanium aluminides, J. Mater. Sci. 36 (2001) 5537-5542.

[4] F. Zhang, L. Lu, M.O. Lai, Grain growth and recrystallization of nanocrystalline Al_3Ti prepared by mechanical alloying, J. Mater. Sci. 38 (2003) 613-619.

[5] T. Wang, J. Zhang, Thermoanalytical and metallographical investigations on the synthesis of $TiAl_3$ from elementary powders, Mater. Chem. Phys. 99 (2006) 20-25.

[6] E.B. Tochaee, H.R.M. Hosseini, S.M.S. Reihani, Fabrication of high strength in-situ Al-Al_3Ti nanocomposite by mechanical alloying and hot extrusion: investigation of fracture toughness, Mater. Sci. Eng. A 658 (2016) 246-254.

[7] Z. Liu, Q. Han, J. Li, Fabrication of in situ Al_3Ti/Al composites by using ultrasound assisted direct reaction between solid Ti powders and liquid Al, Powder Technol. 247 (2013) 55-59.

[8] J. Qin, G. Chen, X. Ji, X. Song, N. Hu, F. Han, Z. Du, Effect of reaction temperature on the microstructures and mechanical properties of high-intensity ultrasonic assisted in-situ Al_3Ti/2024 Al composites, J. Alloy. Compd. 666 (2016)

58-64.

[9] Y. Fu, R. Shi, J. Zhang, J. Sun, G. Hu, Microstructure and mechanical behavior of a multiphase Al_3Ti-based intermetallic alloy, Intermetallics 8 (2000) 1251-1256.

[10] M.V. Karpets, Y.V. Milman, O.M. Barabash, N.P. Korzhova, O.N. Senkov, D.B. Miracle, T.N. Legkaya, I.V. Voskoboynik, The influence of Zr alloying on the structure and properties of Al_3Ti, Intermetallics 11 (2003) 241-249.

[11] T. Wang, Y. Lu, M. Zhu, J. Zhang, Identification of the comprehensive kinetics of thermal explosion synthesis Ti + 3Al → $TiAl_3$ using non-isothermal differential scanning calorimetry, Mater. Lett. 54 (2002) 284-290.

[12] T. Wang, R.Y. Liu, M.L. Zhu, J.S. Zhang, Physical simulation of the effect of sample volume on ignition temperature in the thermal explosion synthesis of Ti + 3Al → $TiAl_3$, Mater. Lett. 57 (2003) 2151-2155.

[13] Q. Zhang, B.L. Xiao, D. Wang, Z.Y. Ma, Formation mechanism of in situ Al_3Ti in Al matrix during hot pressing and subsequent friction stir processing, Mater. Chem. Phys. 130 (2011) 1109-1117.

[14] M. Sujata, S. Bhargava, S. Suwas, S. Sangal, On kinetics of $TiAl_3$ formation during reaction synthesis from solid Ti and liquid Al, J. Mater. Sci. Lett. 20 (2001) 2207-2209.

[15] G.Z. Chen, D.J. Fray, T.W. Farthing, Direct electrochemical reduction of titanium dioxide to titanium in molten calcium chloride, Nature 407 (2000) 361-364.

[16] A.M. Abdelkader, K.T. Kilby, A. Cox, D.J. Fray, DC voltammetry of electro-deoxidation of solid oxides, Chem. Rev. 113 (2013) 2863-2886.

[17] K.S. Mohandas, Direct electrochemical conversion of metal oxides to metal by molten salt electrolysis: a review, Miner. Process. Extr. Metall. Rev. 122 (2014) 195-212.

[18] R. Bhagat, D. Dye, S.L. Raghunathan, R.J. Talling, D. Inman, B.K. Jackson, K.K. Rao, R.J. Dashwood, In situ synchrotron diffraction of the electrochemical reduction pathway of TiO_2, Acta Mater. 58 (2010) 5057-5062.

[19] C. Schwandt, D.J. Fray, Determination of the kinetic pathway in the electrochemical reduction of titanium dioxide in molten calcium chloride, Electrochim. Acta 51 (2005) 66-76.

[20] D.S.M. Vishnu, J. Sure, K.S. Mohandas, Corrosion of high density graphite anodes during direct electrochemical de-oxidation of solid oxides in molten $CaCl_2$ medium, Carbon 93 (2015) 782-792.

[21] U.B. Pal, D.E. Woolley, G.B. Kenney, Emerging SOM technology for the green synthesis of metals from oxides, JOM 53 (2001) 32-35.

[22] U.B. Pal, A.C. Powell IV, The use of solid-oxide-membrane technology for electrometallurgy, JOM 59 (2007) 44-49.

[23] A. Martin, J.C. Poignet, J. Fouletier, M. Allibert, D. Lambertin, G. Bourgès, Yttria-stabilized zirconia as membrane material for electrolytic deoxidation of $CaO–CaCl_2$ melts, J. Appl. Electrochem. 40 (2009) 533-542.

[24] A. Krishnan, X.G. Lu, U.B. Pal, Solid oxide membrane process for magnesium production directly from magnesium oxide, Metall. Mater. Trans. B 36 (2005) 463-473.

[25] X. Zou, X. Lu, Z. Zhou, C. Li, Direct electrosynthesis of Ti_5Si_3/TiC composites from their oxides/C precursors in molten calcium chloride, Electrochem. Commun. 21 (2012) 9-13.

[26] A. Krishnan, X.G. Lu, U.B. Pal, Solid oxide membrane (SOM) technology for environmentally sound production of tantalum metal and alloys from their oxide sources, Scand. J. metall. 34 (2005) 293-301.

[27] X. Lu, X. Zou, C. Li, Q. Zhong, W. Ding, Z. Zhou, Green electrochemical process solid-oxide oxygen-ion-conducting membrane (SOM): direct extraction of Ti-Fe alloys from natural ilmenite, Metall. Mater. Trans. B 43 (2012) 503-512.

[28] X. Zou, X. Lu, C. Li, Z. Zhou, A direct electrochemical route from oxides to Ti–Si intermetallics, Electrochim. Acta 55 (2010) 5173-5179.

[29] X. Zou, X. Lu, Z. Zhou, C. Li, W. Ding, Direct selective extraction of titanium silicide Ti_5Si_3 from multi-component Ti-bearing compounds in molten salt by an electrochemical process, Electrochim. Acta 56 (2011) 8430-8437.

[30] X. Zou, K. Zheng, X. Lu, Q. Xu, Z. Zhou, Solid oxide membrane-assisted controllable electrolytic fabrication of metal carbides in molten salt, Faraday Discuss. 190 (2016) 53-69.

[31] D. Wang, X. Jin, G.Z. Chen, Solid state reactions: an electrochemical approach in molten salts, Annu. Rep. Prog. Chem., Sect. C 104 (2008) 189-234.

[32] W. Xiao, X. Wang, H. Yin, H. Zhu, X. Mao, D. Wang, Verification and implications of the dissolution–electrodeposition process during the electro-reduction of solid silica in molten $CaCl_2$, RSC Adv. 2 (2012) 7588-7593.

[33] Y. Deng, D. Wang, W. Xiao, X. Jin, X. Hu, G.Z. Chen, Electrochemistry at conductor/insulator/electrolyte three-phase interlines: a thin layer model, J. Phys. Chem. B 109 (2005) 14043-14051.

[34] W. Xiao, X. Jin, Y. Deng, D. Wang, X. Hu, G.Z. Chen, Electrochemically driven three-phase interlines into insulator compounds: electroreduction of solid SiO_2 in molten $CaCl_2$, Chemphyschem 7 (2006) 1750-1758.

[35] D. Hu, W. Xiao, G.Z. Chen, Near-Net-Shape Production of Hollow Titanium Alloy Components *via* Electrochemical Reduction of Metal Oxide Precursors in Molten Salts, Metall. Mater. Trans. B 44 (2013) 272-282.

[36] H.Q. Che, Q.C. Fan, Microstructural evolution during the ignition/quenching of pre-heated Ti/3Al powders, J. Alloy. Compd. 475 (2009) 184-190.

[37] X. Jiao, X. Wang, X. Kang, P. Feng, L. Zhang, J. Wang, F. Akhtar, Hierarchical porous $TiAl_3$ intermetallics synthesized by thermal explosion with a leachable space-holder material, Mater. Lett. 181 (2016) 261-264.

[38] D.T.L. Alexander, C. Schwandt, D.J. Fray, Microstructural kinetics of phase transformations during electrochemical reduction of titanium dioxide in molten calcium chloride, Acta Mater. 54 (2006) 2933-2944.

[39] D.T.L. Alexander, C. Schwandt, D.J. Fray, The electro-deoxidation of dense titanium dioxide precursors in molten calcium chloride giving a new reaction pathway, Electrochim. Acta 56 (2011) 3286-3295.

[40] K. Dring, R. Dashwood, D. Inman, Voltammetry of titanium dioxide in molten calcium chloride at 900 °C, J. Electrochem. Soc. 152 (2005) E104-E113.

[41] R.O. Suzuki, M. Aizawa, K. Ono, Calcium-deoxidation of niobium and titanium in Ca-saturated $CaCl_2$ molten salt, J. Alloy. Compd. 288 (1999) 173-182.

[42] M. Ma, D. Wang, W. Wang, X. Hu, X. Jin, G.Z. Chen, Extraction of titanium from different titania precursors by the FFC Cambridge process, J. Alloy. Compd. 420 (2006) 37-45.

[43] S. Tan, T. Örs, M.K. Aydınol, T. Öztürk, İ. Karakaya, Synthesis of FeTi from mixed oxide precursors, J. Alloy. Compd. 475 (2009) 368-372.

[44] X. Zou, X. Lu, Z. Zhou, W. Xiao, Q. Zhong, C. Li, Electrochemical extraction of Ti_5Si_3 silicide from multicomponent Ti/Si-containing metal oxide compounds in molten salt, W. Ding, J. Mater. Chem. A 2 (2014) 7421-7430.

[45] K. Chen, Y. Hua, C. Xu, Q. Zhang, C. Qi, Y. Jie, Preparation of TiC/SiC composites from Ti-enriched slag by an electrochemical process in molten salts, Ceram. Int. 41 (2015) 11428-11435.

Table and Figure Captions

Table 1 The chemical composition of the titanium-rich slag (wt %).

Components	TiO_2	SiO_2	CaO	Al_2O_3	MgO	Total FeO_x	MnO
Content	70.74	6.46	2.58	2.72	3.66	12.56	1.28

Fig. 1. The schematic illustration of the experimental apparatus and the SOM-assisted electro-deoxidation process.

Fig. 2. XRD patterns of the TiO_2/Al_2O_3 mixture precursor before and after being immersed into molten $CaCl_2$ for 2 h.

Fig. 3. XRD patterns of the products obtained from the TiO_2/Al_2O_3 mixture pellet after being electrolyzed for different times.

Fig. 4. (a) The schematic illustration of the partially reduced TiO_2/Al_2O_3 mixture pellet which was firstly ground and then analyzed by XRD; (b) XRD patterns of the partially reduced pellet from the surface to the centre; (c) a schematic illustration of the phase composition of the partially reduced pellet.

Fig. 5. (a) SEM image of the section of the TiO_2/Al_2O_3 mixture pellet after being electrolyzed for 3 h; (b) EDX line profiles of the corresponding position of the SEM image (marked with line in (a)); (c)-(f) The corresponding elemental maps of the

SEM image; (g) (h) SEM images of the outer part (g) and the inner part (h) of the partially reduced pellet.

Fig. 6. (a) SEM image of the product obtained from the TiO_2/Al_2O_3 mixture pellet after 6 h electrolysis, and the inset is the EDX spectrum measured over the SEM imaging area; (b) the enlarged view of the corresponding region marked in (a).

Fig. 7. The schematic illustration of the electrochemical preparation of porous $TiAl_3$ from TiO_2/Al_2O_3 mixture precursor with the use of NaCl as the space-holder material.

Fig. 8. (a) SEM image of the electrochemically prepared $TiAl_3$ without the addition of NaCl; (b) and (c) SEM images of the electrochemically prepared porous $TiAl_3$ with the addition of NaCl; (d) the enlarged view of the corresponding region marked with rectangle in (c).

Fig. 9. The schematic illustration of the reaction mechanism of the electrochemical deoxidation of TiO_2/Al_2O_3 mixture precursor to $TiAl_3$ intermetallic.

Fig. 10. (a) XRD patterns of the initial titanium-rich slag and the mixed titanium-rich/Al_2O_3 before electrolysis, as well as the products obtained from titanium-rich slag/Al_2O_3 mixture pellet after being electrolyzed for different times; (b) the detailed XRD patterns corresponding to the area marked in (a).

Fig. 11. XRD patterns the partially reduced titanium-rich/Al_2O_3 mixture pellet from the pellet's surface to its centre.

Fig. 12. (a) SEM image of initial titanium-rich slag, and the inset is its corresponding EDX spectrum; (b) SEM image of the mixed titanium-rich slag/Al_2O_3; (c) SEM image of the product obtained from the titanium-rich slag/Al_2O_3 mixture pellet after being electrolyzed for 5 h, and the inset is the corresponding EDX spectrum; (d) EDX spectra measured at the corresponding positions marked with rectangles in (c).

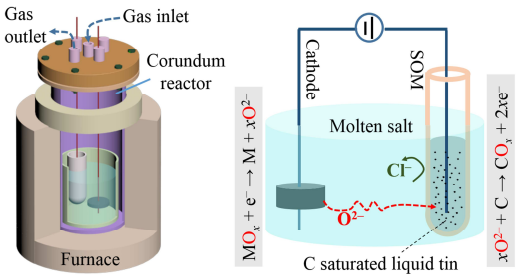

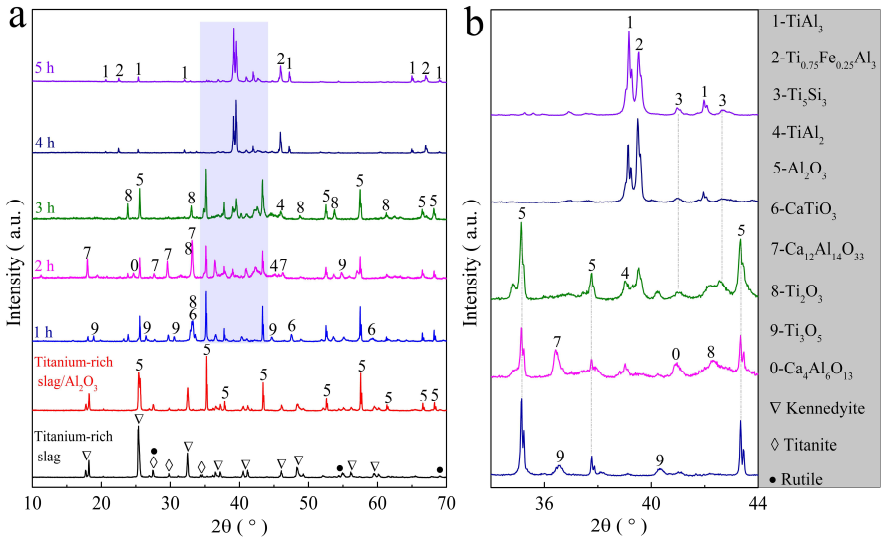

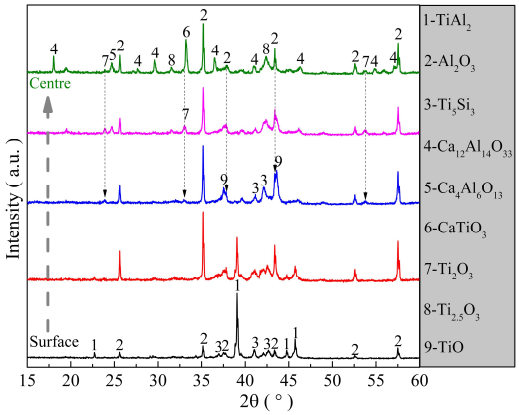

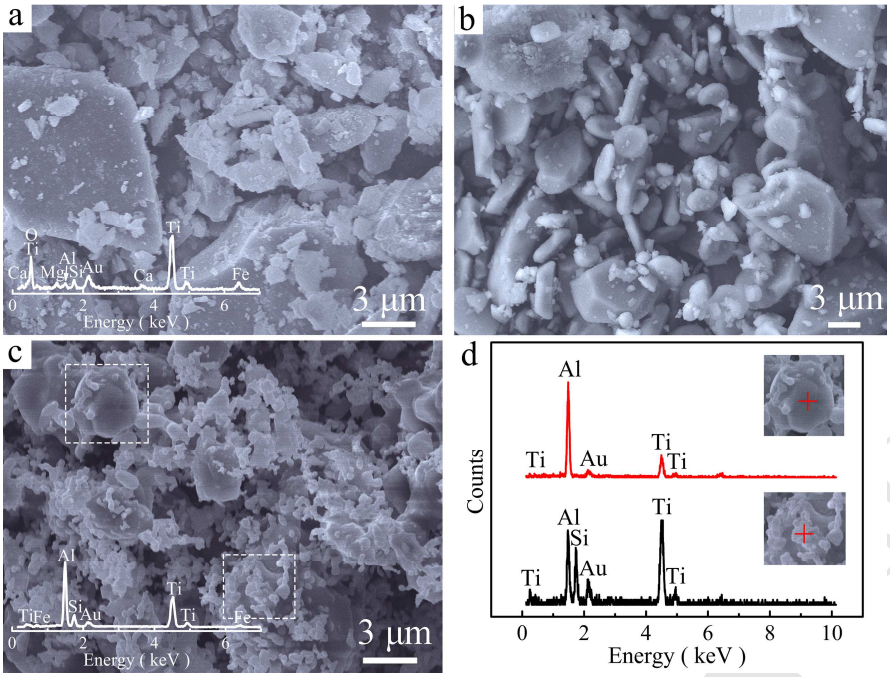

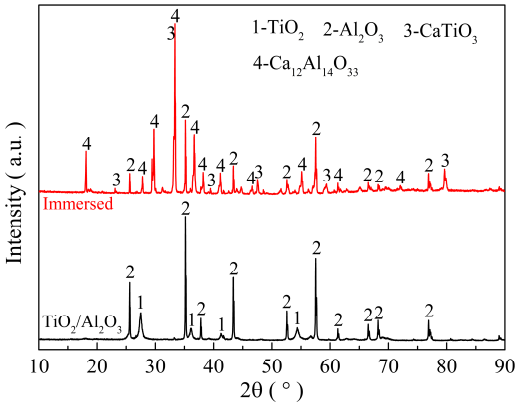

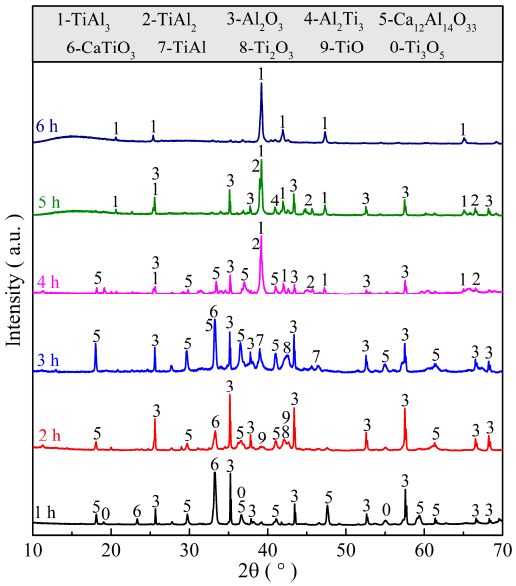

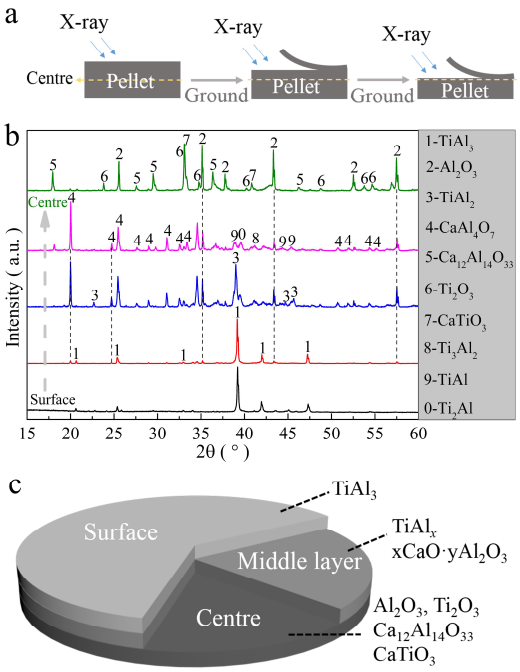

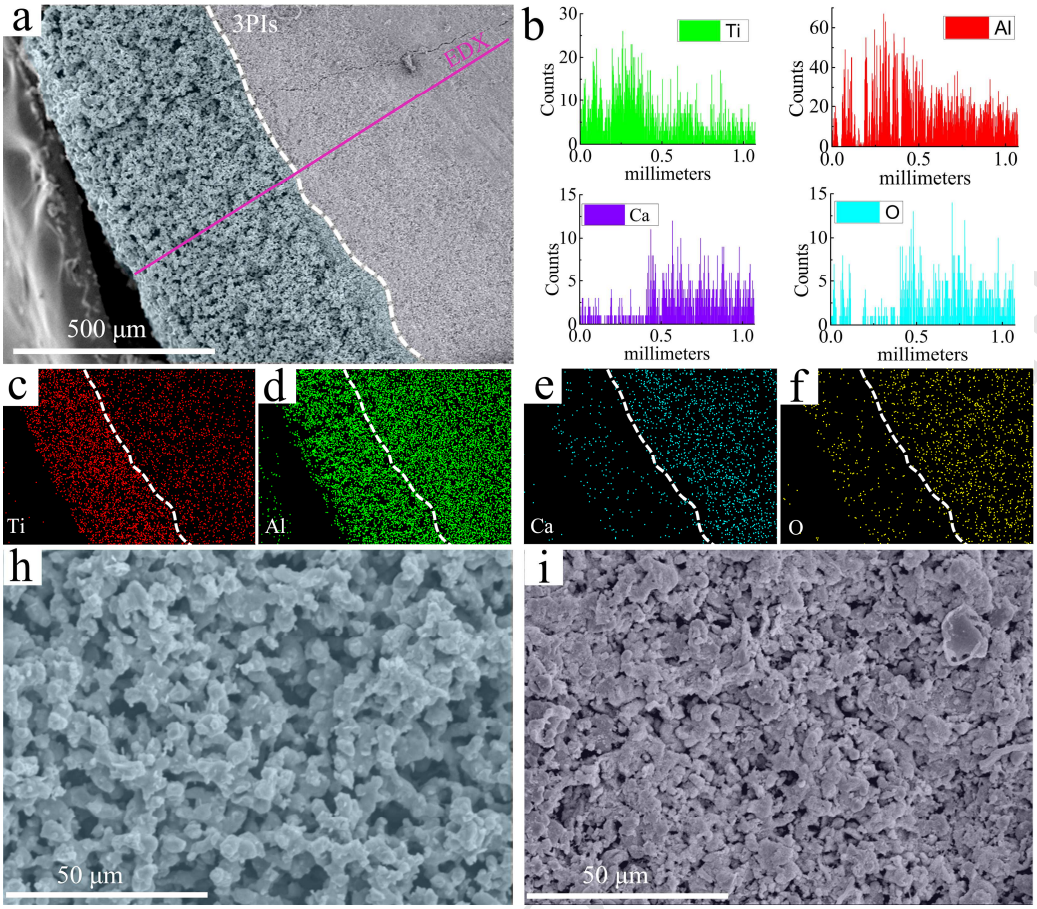

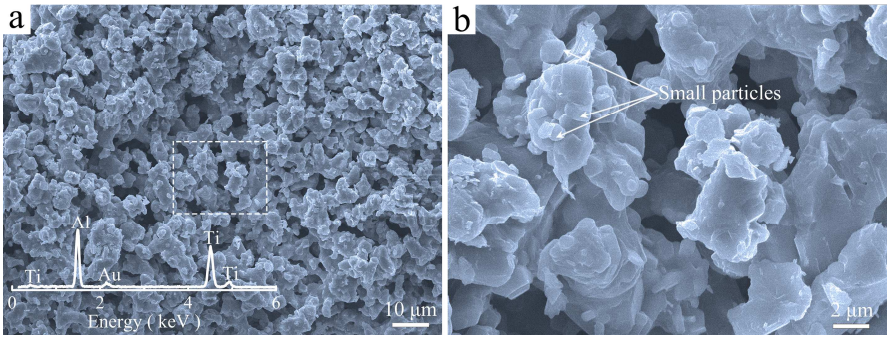

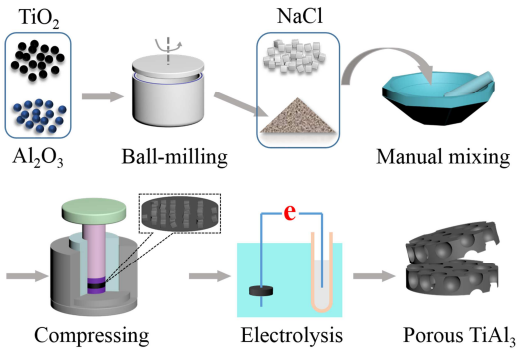

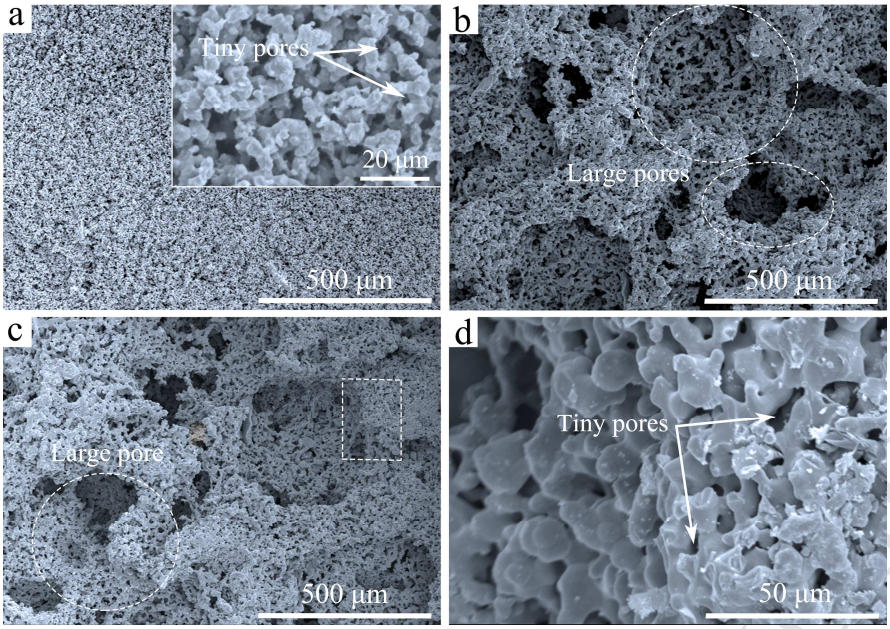

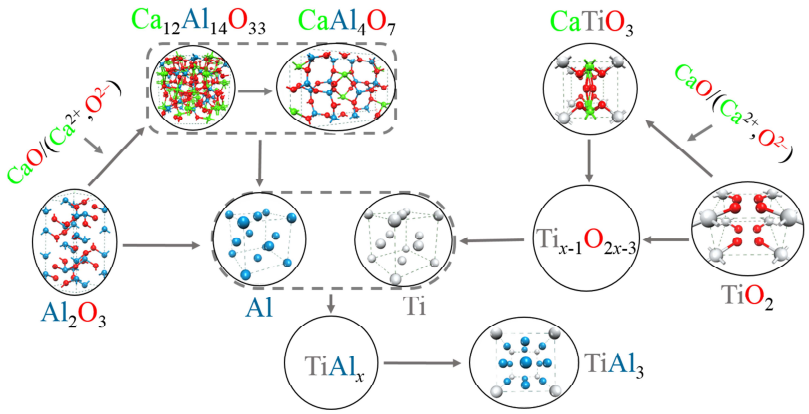

Highlights

(*i*) Direct electrosynthesis of $TiAl_3$ from complex Ti/Al-containing compounds has been investigated.

(*ii*) The reaction mechanism and the detailed reduction process have been determined.

(*iii*) Porous $TiAl_3$ has been produced using the solid oxide oxygen-ion-conducting membrane (SOM) process.